Germline deletion of the miR-17~92 cluster causes skeletal and growth defects in humans

Loïc de Pontual[1,2,10], Evelyn Yao[3,10], Patrick Callier[4], Laurence Faivre[4], Valérie Drouin[5], Sandra Cariou[1], Arie Van Haeringen[6], David Geneviève[7], Alice Goldenberg[5], Myriam Oufadem[1], Sylvie Manouvrier[8], Arnold Munnich[1,9], Joana Alves Vidigal[3], Michel Vekemans[1], Stanislas Lyonnet[1,9], Alexandra Henrion-Caude[1], Andrea Ventura[3,10] & Jeanne Amiel[1,9,10]

MicroRNAs (miRNAs) are key regulators of gene expression in animals and plants. Studies in a variety of model organisms show that miRNAs modulate developmental processes. To our knowledge, the only hereditary condition known to be caused by a miRNA is a form of adult-onset non-syndromic deafness[1], and no miRNA mutation has yet been found to be responsible for any developmental defect in humans. Here we report the identification of germline hemizygous deletions of *MIR17HG*, encoding the miR-17~92 polycistronic miRNA cluster, in individuals with microcephaly, short stature and digital abnormalities. We demonstrate that haploinsufficiency of miR-17~92 is responsible for these developmental abnormalities by showing that mice harboring targeted deletion of the miR-17~92 cluster phenocopy several key features of the affected humans. These findings identify a regulatory function for miR-17~92 in growth and skeletal development and represent the first example of an miRNA gene responsible for a syndromic developmental defect in humans.

The *MIR17HG* locus encodes for miR-17~92, a polycistronic miRNA cluster from which six distinct miRNAs are produced (**Supplementary Fig. 1**). Genetic and functional studies have provided overwhelming evidence that this cluster is a bona fide human oncogene[2–10]. In addition, loss-of-function experiments in mice have shown that miR-17~92 is essential for mammalian development and that its complete inactivation leads to perinatal lethality[11].

Feingold syndrome (MIM164280) is an autosomal dominant syndrome whose core features are microcephaly, relative short stature and digital anomalies, particularly brachymesophalangy of the second and fifth fingers and brachysyndactyly of the toes[12,13]. Less penetrant defects include oesophageal, duodenal atresia (observed in 30–55% of cases), heart and kidney defects and variable learning disabilities. In approximately 70% of affected families, Feingold syndrome is caused by germline loss-of-function mutations of *MYCN* (MIM164840) at 2p24.1 (refs. 14,15), but the genetic lesion(s) responsible for the remaining cases have yet to be identified.

We employed high-resolution comparative genomic hybridization (CGH) arrays to perform a genome-wide analysis of ten index subjects with skeletal abnormalities consistent with a diagnosis of Feingold syndrome but who lacked any mutation at the *MYCN* locus (**Supplementary Table 1**). This led to the identification of germline hemizygous microdeletions at 13q31.3 in two subjects (AO39 II3 and AO70 II1; **Figs. 1** and **2a**). The deletion in AO39 II3 spans 2.98 Mb and encompasses three genes: *LOC144776*, *MIR17HG* and *GPC5* (*Glypican-5*). The deletion identified in AO70 II1 is more informative, as it spans 165 kb and encompasses only miR-17~92 and the first exon of *GPC5* (**Fig. 2a**). Quantitative PCR (qPCR) and direct sequencing of *MIR17HG* (including the promoter region) and of the *GPC5* coding sequence failed to identify non-annotated sequence variations in the remaining eight index subjects (data not shown, and the primers used are listed in **Supplementary Table 2**).

By genomic qPCR, we determined that the deletions detected in the two index subjects segregate with disease in the two families (**Fig. 2b**), thus lending support to the hypothesis that these two microdeletions are the causative mutations in these individuals. Next, we queried the Database of Chromosomal Imbalance and Phenotype in Humans Using Ensembl Resources (DECIPHER) database, which contains array CGH data from more than 6,000 individuals with a variety of disorders[16], and identified an additional individual (subject id: 248412) harboring a 180-kb hemizygous 13q31.3 microdeletion encompassing the entire *MIR17HG* locus and the first exon of *GPC5* (**Figs. 1** and **2a**). This deletion was further confirmed by genomic qPCR (**Fig. 2b**). Unfortunately, because of the lack of any genetic and clinical data from the parents of this individual, it is unclear whether the deletion was inherited or was *de novo*. Although not classified as having Feingold syndrome, this

[1]Unité INSERM U-781, Université Paris Descartes, Paris, France. [2]Services de Pédiatrie, Hôpital Jean Verdier, Université Paris XIII, Assistance Publique-Hôpitaux de Paris (AP-HP), Bondy, France. [3]Cancer Biology and Genetics Program, Memorial Sloan-Kettering Cancer Center, New York, New York, USA. [4]Service de Génétique, Hôpital d'enfants, Dijon, France. [5]Service de Génétique, Hôpital Charles Nicolle, Rouen, France. [6]Department of Human and Clinical Genetics, Leiden University Medical Center, Leiden, The Netherlands. [7]Service de Génétique, Hôpital Arnaud de Villeneuve, Montpellier, France. [8]Service de Génétique Clinique, Hôpital J. de Flandre, Lille, France. [9]Services de Génétique et Cytogénétique, Hôpital Necker-Enfant Malades, AP-HP, Paris, France. [10]These authors contributed equally to this work. Correspondence should be addressed to J.A. (jeanne.amiel@inserm.fr) or A.V. (venturaa@mskcc.org).

Received 12 April; accepted 29 July; published online 4 September 2011; doi:10.1038/ng.915

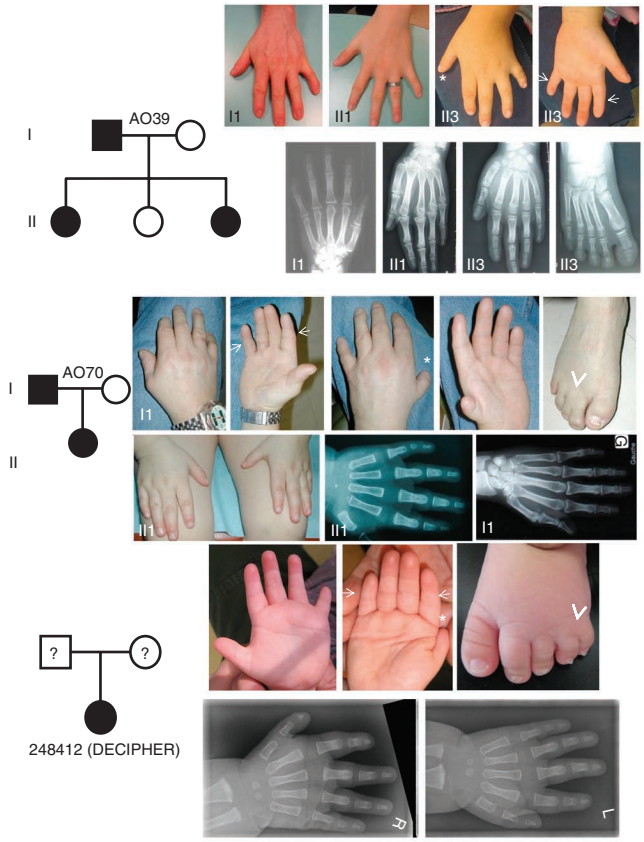

Figure 1 Clinical features of individuals with 13q31.3 deletions. Clinical features and radiographs of affected individuals from families AO39 and AO70 and subject 248412 showing brachydactyly, brachymesophalangy of the second and fifth fingers (better appreciated on the palmar view, arrows), hypoplastic thumbs of variable severity (asterisks) and cutaneous syndactyly of toes (arrow heads).

subject has a combination of features compatible with a diagnosis of Feingold syndrome (**Fig. 1** and **Supplementary Table 1**). The only exception to this was the presence of unusually hypoplastic thumbs, a trait we also observed in the affected father from family AO70 (**Fig. 1** and **Supplementary Table 1**) and one that is rarely as severe in individuals with Feingold syndrome with mutations in *MYCN*[15]. Analogous digital abnormalities were previously reported in some individuals with large 13q deletions[17,18]; however, because of the large size of the deletions, the gene(s) responsible for the developmental defects could not be identified.

To determine whether hemizygous loss of *MIR17HG* in humans results in a detectable reduction of miR-17~92 expression, we performed RT-qPCR on total RNA extracted from white blood cells obtained from three individuals carrying the 13q31.3 microdeletions. In these individuals, expression of all six miRNAs encoded by the miR-17~92 cluster was approximately 50% relative to control individuals (**Fig. 2c**). This indicates that hemizygous loss of miR-17~92 results in a substantial reduction in the expression of its constituent miRNAs that is not compensated by upregulation of the remaining allele.

Together, these findings suggest that hemizygous deletion of *MIR17HG* and/or *GPC5* is responsible for the skeletal abnormalities observed in these subjects, but they do not define the relative contribution of either gene. To address this issue, we first queried the Database of Genomic Variants[19], which compiles structural variations detected in the genomes of healthy individuals (see URLs). We identified two Yoruba control individuals[20] heterozygous for a deletion encompassing exon 4 of *GPC5* (**Supplementary Fig. 2**), which is predicted to produce a loss-of-function allele, as exon 3 and exon 5 are not in frame. Moreover, the 1000 Genomes browser (see URLs) reports a single nucleotide insertion in the coding sequence of *GPC5* (rs34433071, c.1356_1357insC, p.Val454Cys*fs*X7). Although the allelic frequency of this variant is currently unknown, the insertion is predicted to result in the loss of the 113 C-terminal amino acids of GPC5. In contrast, although a ~1.8-kb deletion ending 1.4 kb upstream of the first miRNA of the miR-17~92 cluster is reported in five normal individuals (**Supplementary Fig. 2**), we identified no structural variants or polymorphisms directly affecting the miRNAs encoded by the cluster in these databases. Collectively, these data indicate that hemizygous loss of *GPC5* alone cannot account for the phenotypes observed in our subjects. To determine whether miR-17~92 haploinsufficiency can explain some of the defects observed in individuals harboring 13q31.1 microdeletions, we next examined the consequences of hemizygous deletion of this cluster in mice[11].

Animals harboring targeted deletions of a single miR-17~92 allele (miR-17~92$^{\Delta/+}$) are viable and fertile but are significantly smaller than wild-type controls[11] (**Fig. 3a**), a feature also observed in both

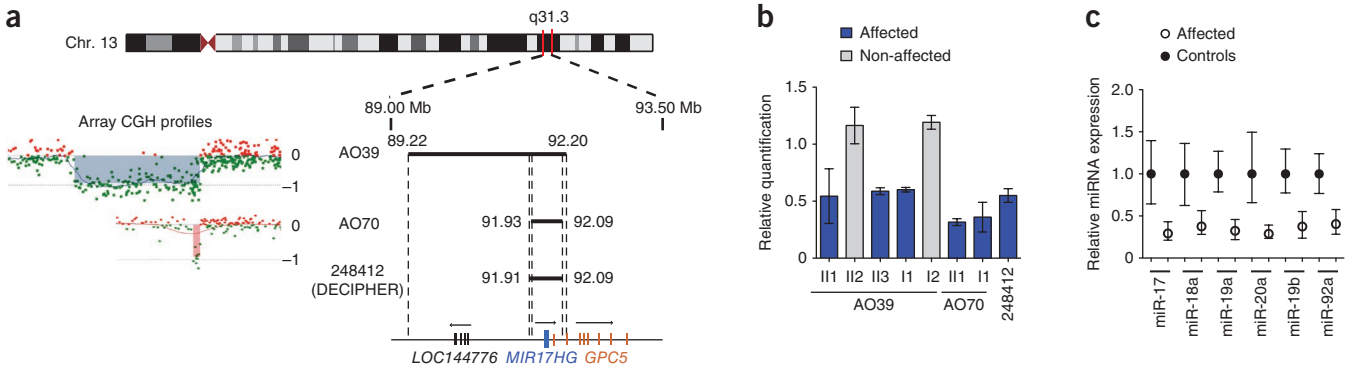

Figure 2 Mapping 13q31.3 microdeletions in individuals with Feingold syndrome. (**a**) Schematic illustration of the microdeletions identified in families AO39 and AO70 and in individual 248412 from DECIPHER. (**b**) Genomic qPCR showing that the microdeletion segregates with disease in families AO70 and AO39. (**c**) RT-qPCR showing reduced expression of individual miRNAs encoded by the miR-17~92a cluster in peripheral white blood cells of individuals carrying 13q31.3 microdeletions ($n = 3$) compared to healthy donors ($n = 4$). For each miRNA, the mean relative expression and the range of expression (error bars) compared to control donors are shown.

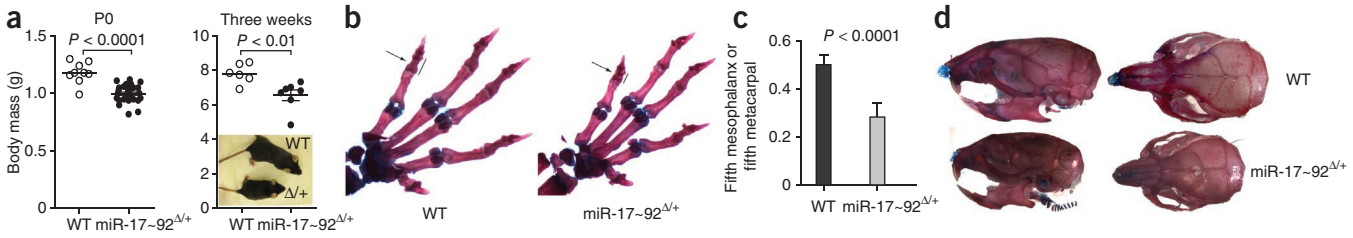

Figure 3 miR-17~92$^{\Delta/+}$ mice display features of Feingold syndrome. (**a**) Mice hemizygous for miR-17~92 are smaller than their wild-type littermates. We weighed wild-type (empty circles) and miR-17~92$^{\Delta/+}$ (filled circles) mice at postnatal day 0 (P0) (left panel) or at weaning (3 weeks, right panel). We computed *P* values using a two-tailed *t*-test. (**b**) Alcian blue and alizarin red staining of wild-type and miR-17~92$^{\Delta/+}$ forelimbs from female age-matched mice. The fifth mesophalanx (arrows) is shorter in hemizygous animals compared to wild-type mice (bar). (**c**) Quantification of the relative length of the fifth mesophalanx in wild-type ($n = 6$) and miR-17~92$^{\Delta/+}$ ($n = 10$) mouse forelimbs. The ratio between the length of the fifth mesophalanx and the length of the fifth metacarpal bone is plotted. Error bars, s.d. (**d**) Lateral (left) and dorsal (right) views of mouse skulls of age-matched wild-type (top) and miR-17~92$^{\Delta/+}$ (bottom) male mice.

individuals with Feingold syndrome with mutations in *MYCN* and individuals harboring 13q31.3 microdeletions. Skeletal analysis of the limbs from age- and sex-matched wild-type and miR-17~92$^{\Delta/+}$ adult mice revealed a striking shortening of the mesophalanx of the fifth finger in heterozygous animals (**Fig. 3b**,**c**), another feature observed in individuals with 13q31.3 microdeletions and in virtually all individuals with Feingold syndrome[15]. Other long bones in the hands of miR-17~92$^{\Delta/+}$ mice were only marginally shorter than in wild-type mice (**Fig. 3b** and data not shown), and we did not observe syndactyly in any of the hemizygous animals. Analysis of the skulls of miR-17~92$^{\Delta/+}$ mice revealed shortening of the anterior-posterior axis and an overall reduction in size, which are both consistent with microcephaly (**Fig. 3d**). Notably, though *Gpc5* and miR-17~92 are also closely linked in the mouse genome, targeted deletion of miR-17~92 does not negatively affect the expression of *Gpc5* in the forelimbs of developing mouse embryos or in mouse embryo fibroblasts (**Supplementary Fig. 3** and data not shown), further showing that miR-17~92, but not Gpc5, is responsible for the key features observed in miR-17~92$^{\Delta/+}$ mice and in individuals harboring 13q31.3 deletions.

Prompted by these findings, we examined the consequences of complete loss of miR-17~92 function on skeletal development. Because homozygous deletion of the cluster leads to perinatal lethality in mice[11], we analyzed animals at embryonic day 18.5 (E18.5). Skeletal preparations of miR-17~92$^{\Delta/\Delta}$ embryos revealed a severe and general delay of endochondral and membranous ossification (**Fig. 4**). Notably, the main limb defects observed in individuals with Feingold syndrome were grossly exacerbated in these animals. More specifically, we observed the complete absence of the mesophalanx of the fifth digit, the presence of a small mesophalanx of the second digit and hypoplasia of the first digital ray (**Fig. 4a** and **Supplementary Fig. 4**). In addition, all embryos examined presented with fusion of the cervical vertebrae (**Fig. 4b** and **Supplementary Fig. 4**) and microcephaly (**Fig. 4c**,**d**). Additional skeletal defects consistently observed in these embryos included dysmorphic zeugopods and fusion of the proximal carpal bones (**Fig. 4a** and **Supplementary Fig. 4**). In sum, the human genetic data and the analysis of miR-17~92$^{\Delta/\Delta}$ and miR-17~92$^{\Delta/+}$ mice show that miR-17~92 haploinsufficiency is responsible for developmental abnormalities in humans and highlight a previously unappreciated role for miR-17~92 in normal growth and skeletal development.

Based on the similarities between the skeletal defects observed in individuals with Feingold syndrome harboring *MYCN* mutations and in individuals with hemizygous deletion of *MIR17HG*, it is tempting to speculate that these two genes may be components of the same developmental pathways and that miR-17~92 may be an important target of MYCN in skeletal development. Indeed, several lines of evidence indicate a close genetic and functional interaction between the MYC family of transcription factors (MYC, MYCN and MYCL)

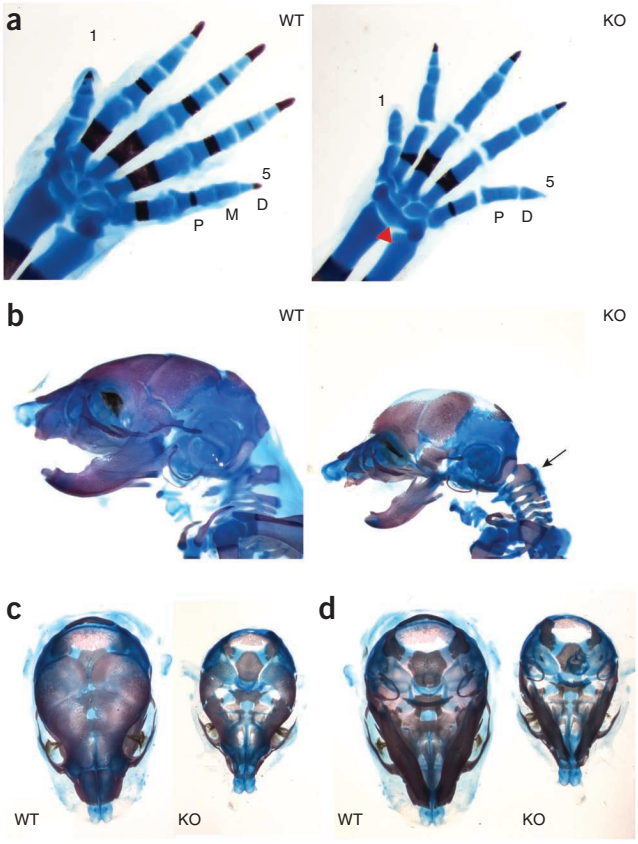

Figure 4 Widespread skeletal defects in E18.5 miR-17~92$^{\Delta/\Delta}$ embryos. (**a**) Skeletal staining of the left hand of E18.5 littermate embryos. Notice the absence of the fifth mesophalanx (M) in the forelimb of the miR-17~92$^{\Delta/\Delta}$ embryo (P, proximal; D, distal). Also notice the delayed ossification of the metacarpal bones and proximal phalanges and the fusion of the first row of carpal bones (red arrowhead) in the mutant embryo. (**b**) Lateral views of embryonic skeletons showing delayed ossification of the skull and asymmetric fusions of the first three cervical vertebrae in the knockout animals (arrow). Dorsal (**c**) and ventral (**d**) views of the skulls of miR-17~92$^{\Delta/\Delta}$ and wild-type E18.5 embryos showing microcephalia and delayed ossification of occipital, parietal and frontal bones in mutant embryos.

and the miR-17~92 cluster. Both MYC and MYCN can activate the transcription of miR-17~92 (refs. 2,6,21–23, **Supplementary Fig. 5** and **Supplementary Note**) and can directly bind to the miR-17~92 promoter region in human and murine cells[21,23,24] (**Supplementary Fig. 6**). Furthermore, ectopic expression of miR-17~92 cooperates with *Myc* in murine models of B-cell lymphoma and colorectal cancer[4,25]. A possible cooperation between MYCN and miR-17~92 in modulating developmental processes is further supported by the remarkable similarity of the phenotypes observed in miR-17~92$^{\Delta/\Delta}$ mice and in mice carrying hypomorphic or null *Mycn* alleles (**Supplementary Table 3**)[26–28].

One hypothesis emerging from these observations is that MYCN regulates various aspects of mammalian development through transactivation of miR-17~92. This hypothesis can be further refined by considering the phenotypic differences between mice carrying mutant alleles of *Mycn* and miR-17~92 and by comparing the consequences of *MYCN* and miR-17~92 loss in affected humans. For example, although individuals with Feingold syndrome with *MYCN* haploinsufficiency frequently present with gastrointestinal atresia (55% of cases)[15], we did not observe this phenotype in any of the six individuals with mutant miR-17~92 described here nor did we observe it in miR-17~92$^{\Delta/+}$ or miR-17~92$^{\Delta/\Delta}$ mice (data not shown). Because abnormal gut development is reported in *Mycn*$^{\Delta/\Delta}$ mice[29,30] (**Supplementary Table 3**), it seems plausible that MYCN controls gastrointestinal development independently of miR-17~92 or that miR-17~92 is functionally redundant. In contrast, microcephaly, short stature and brachymesophalangy are seen in humans and mice with mutated *MYCN* or miR-17~92, indicating functional cooperation between these two genes in skeletal development and growth.

Because none of the individuals with an *MIR17HG* deletion have gastrointestinal atresia, whether they should be classified as true cases of Feingold syndrome or as affected by a new form of brachydactyly with short stature and microcephaly remains an open question. Nevertheless, our results provide a strong rationale for testing all individuals with skeletal features of Feingold syndrome for mutations in both *MYCN* and *MIR17HG*.

At present, the detailed molecular mechanisms and the targets through which miR-17~92 modulates skeletal development remain unknown and will be the subject of future studies. Yet, it is worth noting that miR-17~92 has been shown to modulate the TGF-β and sonic hedgehog axes[6,10,31–33], two of the most important signaling pathways controlling skeletal development and limb patterning.

Although our analysis of miR-17~92$^{\Delta/+}$ mice clearly indicates that reduced dosage of this cluster can generate many of the skeletal phenotypes observed in individuals with Feingold syndrome with *MYCN* mutations and in individuals harboring 13q31.3 microdeletions, we cannot exclude the possibility that *GPC5* haploinsufficiency also contributes to the pathogenesis of some of these phenotypes. In particular, it is possible that *GPC5* haploinsufficiency plays a role in the severe thumb hypoplasia observed in some individuals carrying 13q31.3 microdeletions. Addressing this issue will require the identification and characterization of additional families carrying deletions of this region and the generation of miR-17~92 and *Gpc5* compound-mutant animals.

In conclusion, this study provides the first evidence, to our knowledge, of a germline mutation of an miRNA gene leading to a developmental defect in humans. Together with the previous report of mutation of miR-96 in adult-onset hereditary deafness[1], miR-17~92 represents the only other known example of an miRNA directly responsible for a hereditary disease in humans. Our results also expand the known biological activities of a major oncogenic miRNA cluster by showing its role in skeletal growth and patterning and suggest a possible functional interaction between *MYCN* and miR-17~92 in modulating embryonic development.

URLs. OMIM, http://www.ncbi.nlm.nih.gov/omim/; Ensembl, http://useast.ensembl.org/index.html; Database of Genomic Variants, http://projects.tcag.ca/variation/; 1000 Genomes Browser, http://browser.1000genomes.org/index.html; UCSC Genome Assembly, http://genome.ucsc.edu/.

METHODS

Methods and any associated references are available in the online version of the paper at http://www.nature.com/naturegenetics/.

Note: Supplementary information is available on the Nature Genetics website.

ACKNOWLEDGMENTS

We are thankful to the subjects and their referent doctors for their active participation in this study. We are also particularly thankful to P. Hurlin for generously providing forelimbs of *Mycn* conditional knockout mouse embryos. This work was supported by grants from the Agence Nationale de la Recherche (ANR grant EvoDevoMut), the Foundation pour la Recherche Médicale (FRM), the Institut National du Cancer-Direction de l'Hospitalisation et de l'Organisation des soins (INCa-DHOS), and the Institut National du Cancer. Work in the laboratory of A.V. was funded by US National Institutes of Health (NIH)-National Cancer Institute (NCI) grant R01CA149707, a Sidney Kimmel Award and a Geoffrey Beene Research Grant. E.Y. is a recipient of the NIH Molecular and Cellular Biology T32 training grant. We thank L. Selleri for her expertise in the phenotypic analysis of miR-17~92–mutant mice skeletons, L. Legeai-Mallet, A. Pelet and P. Ogrodowski for helpful discussion and technical advice and J. Hollenstein for editing the manuscript.

AUTHOR CONTRIBUTIONS

L.d.P., P.C., S.C. and M.O. performed subject-related experiments. E.Y. performed the analysis of miR-17~92 mutant mice, the ChIP experiments and determined miR-17~92 expression in subjects. J.A.V. determined miR-17~92 expression in mouse embryos. J.A. and A.V. designed and supervised the project and wrote the manuscript. A.M., M.V., S.L., L.d.P., E.Y. and A.H.-C. provided critical input into project development and manuscript preparation. All other coauthors identified subjects with Feingold syndrome and performed related clinical and laboratory studies (L.F., V.D., A.V.H., D.G., A.G. and S.M.).

COMPETING FINANCIAL INTERESTS

The authors declare no competing financial interests.

Published online at http://www.nature.com/naturegenetics/.
Reprints and permissions information is available online at http://www.nature.com/reprints/index.html.

1. Mencía, A. *et al.* Mutations in the seed region of human miR-96 are responsible for nonsyndromic progressive hearing loss. *Nat. Genet.* **41**, 609–613 (2009).
2. Fontana, L. *et al.* Antagomir-17–5p abolishes the growth of therapy-resistant neuroblastoma through p21 and BIM. *PLoS ONE* **3**, e2236 (2008).
3. Hayashita, Y. *et al.* A polycistronic microRNA cluster, miR-17–92, is overexpressed in human lung cancers and enhances cell proliferation. *Cancer Res.* **65**, 9628–9632 (2005).
4. He, L. *et al.* A microRNA polycistron as a potential human oncogene. *Nature* **435**, 828–833 (2005).
5. Mu, P. *et al.* Genetic dissection of the miR-17~92 cluster of microRNAs in Myc-induced B-cell lymphomas. *Genes Dev.* **23**, 2806–2811 (2009).
6. Northcott, P.A. *et al.* The miR-17/92 polycistron is up-regulated in sonic hedgehog–driven medulloblastomas and induced by N-myc in sonic hedgehog–treated cerebellar neural precursors. *Cancer Res.* **69**, 3249–3255 (2009).
7. Olive, V. *et al.* miR-19 is a key oncogenic component of mir-17–92. *Genes Dev.* **23**, 2839–2849 (2009).
8. Ota, A. *et al.* Identification and characterization of a novel gene, C13orf25, as a target for 13q31-q32 amplification in malignant lymphoma. *Cancer Res.* **64**, 3087–3095 (2004).
9. Tagawa, H. & Seto, M. A microRNA cluster as a target of genomic amplification in malignant lymphoma. *Leukemia* **19**, 2013–2016 (2005).
10. Uziel, T. *et al.* The miR-17~92 cluster collaborates with the sonic hedgehog pathway in medulloblastoma. *Proc. Natl. Acad. Sci. USA* **106**, 2812–2817 (2009).
11. Ventura, A. *et al.* Targeted deletion reveals essential and overlapping functions of the miR-17 through 92 family of miRNA clusters. *Cell* **132**, 875–886 (2008).
12. Celli, J., van Bokhoven, H. & Brunner, H.G. Feingold syndrome: clinical review and genetic mapping. *Am. J. Med. Genet. A.* **122A**, 294–300 (2003).

13. Feingold, M., Hall, B.D., Lacassie, Y. & Martinez-Frias, M.L. Syndrome of microcephaly, facial and hand abnormalities, tracheoesophageal fistula, duodenal atresia, and developmental delay. *Am. J. Med. Genet.* **69**, 245–249 (1997).
14. van Bokhoven, H. *et al.* MYCN haploinsufficiency is associated with reduced brain size and intestinal atresias in Feingold syndrome. *Nat. Genet.* **37**, 465–467 (2005).
15. Marcelis, C.L. *et al.* Genotype-phenotype correlations in MYCN-related Feingold syndrome. *Hum. Mutat.* **29**, 1125–1132 (2008).
16. Firth, H.V. *et al.* DECIPHER: Database of Chromosomal Imbalance and Phenotype in Humans Using Ensembl Resources. *Am. J. Hum. Genet.* **84**, 524–533 (2009).
17. Morales, J.A., Mendizabal, A.P., Vasquez, A.I., Figuera, L.E. & Gonzalez-Garcia, J.R. Interstitial deletion of 13q22→q31: case report and review of the literature. *Clin. Dysmorphol.* **15**, 139–143 (2006).
18. Quélin, C. *et al.* Twelve new patients with 13q deletion syndrome: genotype-phenotype analyses in progress. *Eur. J. Med. Genet.* **52**, 41–46 (2009).
19. Iafrate, A.J. *et al.* Detection of large-scale variation in the human genome. *Nat. Genet.* **36**, 949–951 (2004).
20. Kidd, J.M. *et al.* Mapping and sequencing of structural variation from eight human genomes. *Nature* **453**, 56–64 (2008).
21. O'Donnell, K.A., Wentzel, E.A., Zeller, K.I., Dang, C.V. & Mendell, J.T. c-Myc-regulated microRNAs modulate E2F1 expression. *Nature* **435**, 839–843 (2005).
22. Schulte, J.H. *et al.* MYCN regulates oncogenic microRNAs in neuroblastoma. *Int. J. Cancer* **122**, 699–704 (2008).
23. Lovén, J. *et al.* MYCN-regulated microRNAs repress estrogen receptor-α (ESR1) expression and neuronal differentiation in human neuroblastoma. *Proc. Natl. Acad. Sci. USA* **107**, 1553–1558 (2010).
24. Chen, X. *et al.* Integration of external signaling pathways with the core transcriptional network in embryonic stem cells. *Cell* **133**, 1106–1117 (2008).
25. Dews, M. *et al.* Augmentation of tumor angiogenesis by a Myc-activated microRNA cluster. *Nat. Genet.* **38**, 1060–1065 (2006).
26. Nagy, A. *et al.* Dissecting the role of N-myc in development using a single targeting vector to generate a series of alleles. *Curr. Biol.* **8**, 661–664 (1998).
27. Moens, C.B., Auerbach, A.B., Conlon, R.A., Joyner, A.L. & Rossant, J. A targeted mutation reveals a role for N-myc in branching morphogenesis in the embryonic mouse lung. *Genes Dev.* **6**, 691–704 (1992).
28. Ota, S., Zhou, Z.Q., Keene, D.R., Knoepfler, P. & Hurlin, P.J. Activities of N-Myc in the developing limb link control of skeletal size with digit separation. *Development* **134**, 1583–1592 (2007).
29. Stanton, B.R., Perkins, A.S., Tessarollo, L., Sassoon, D.A. & Parada, L.F. Loss of N-myc function results in embryonic lethality and failure of the epithelial component of the embryo to develop. *Genes Dev.* **6**, 2235–2247 (1992).
30. Sawai, S. *et al.* Defects of embryonic organogenesis resulting from targeted disruption of the N-myc gene in the mouse. *Development* **117**, 1445–1455 (1993).
31. Mestdagh, P. *et al.* The miR-17–92 microRNA cluster regulates multiple components of the TGF-β pathway in neuroblastoma. *Mol. Cell* **40**, 762–773 (2010).
32. Volinia, S. *et al.* A microRNA expression signature of human solid tumors defines cancer gene targets. *Proc. Natl. Acad. Sci. USA* **103**, 2257–2261 (2006).
33. Dews, M. *et al.* The myc-miR-17~92 axis blunts TGF-β signaling and production of multiple TGF-β-dependent antiangiogenic factors. *Cancer Res.* **70**, 8233–8246 (2010).

ONLINE METHODS

Subjects. Subjects were referred by their clinical geneticists for molecular analysis as possible cases of Feingold syndrome. Informed consent was obtained from all subjects or from their legal tutor. Clinical diagnostic criteria included three or more of the core features for Feingold syndrome, namely: (i) microcephaly, (ii) brachymesophalangy, (iii) facial features compatible with those previously described in individuals with Feingold syndrome and (iv) oesophageal or duodenal atresia. Subjects included in the series had no mutation in the *MYCN* coding sequence and no deletion encompassing the locus[34]. The clinical data for each subject are summarized in **Supplementary Table 1**.

Array comparative genomic hybridization (CGH). Array CGH was performed using the Agilent Human Genome CGH Microarray Kit 105K and 244K (Agilent Technologies)[35]. Array CGH analysis was performed according to the Agilent protocol with the following minor protocol modifications: DNA was labeled by direct incorporation of Cya-5 and Cya-3 using an Oligo-array kit (Enzo) for 4 h and purified using a QIAmp DNA Mini kit (QIAGEN). A graphical overview was obtained using Genomic Workbench software (v5.0) and the statistical algorithm ADM-2 according to a sensitivity threshold of 6.0 and a moving average window of 0.5 Mb. Mapping data were analyzed on the human genome sequence using Ensembl (see URLs). Copy number variations were assessed in the Database of Genomic Variants (see URLS). An Affymetrix 500K was used for the individual quoted in DECIPHER.

Quantitative real-time PCR (qPCR). Blood samples were obtained with informed consent for molecular analysis, and DNA was extracted according to standard protocols. Primers were designed to amplify the pri–miR-17~92 region chosen, and *MYCN* was used as a reference gene (the sequences of the primers are listed in **Supplementary Table 3**). Micro rearrangements in the individual from DECIPHER and from AO39 II3 and AO70 II1 were tested in all available members of the two families by semiquantitative PCR on a Mastercycler Realplex machine (Eppendorf) using the GoTaq qPCR Master Mix protocol.

Total RNA from peripheral white blood cells of affected individuals and healthy controls was extracted using a standard TRIzol protocol. Expression of the miR-17~92 cluster of miRNAs was determined with TaqMan miRNA expression assays (Applied Biosystems) according to the manufacturer's instructions. Samples were assayed in quadruplicate and normalized to sno135.

Mouse husbandry. All animal studies and procedures were approved by the Memorial Sloan-Kettering Cancer Center Institutional Animal Care and Use Committee. Mice were maintained in a mixed 129SvJae and C57/B6 background. miR-17~92$^{\Delta/+}$ and miR-17~92$^{\Delta/\Delta}$ mice have been previously described[11].

Skeletal preparations. E18.5 embryos were eviscerated and soaked in ddH_2O for 3 h at room temperature (17–22 °C). Fetuses were heat shocked in a 65 °C water bath for 1 min to facilitate skinning. Adult mice were killed by CO_2 asphyxiation, skinned and eviscerated. All carcasses were fixed in 100% ethanol and incubated in alcian blue (150 mg/l alcian blue 8GX, 80% ethanol, 20% acetic acid) and alizarin red (50 mg/l alizarin red S in 2% KOH) to stain for cartilage and bone, respectively. Remaining tissues were cleared in 2% KOH-ddH_2O, and skeletons were placed in 25% glycerol-ddH_2O for storage. Images were captured with a Zeiss Stereo Discovery V8 microscope and processed in Photoshop. Images were acquired at the same magnification to allow for direct comparison between different genotypes.

Measurements of digit length were performed in ImageJ, and ratios were determined by measuring the length of the fifth mesophalanx from each limb and normalizing to the fifth metacarpal.

Pri–miR-17~92 and *GPC5* direct sequencing. The PCR reaction mixture (25 µl) contained 100 ng of leukocyte DNA, 20 pmol of each primer (**Supplementary Table 3**), 0.1 µM dNTP and 1 U *Taq* DNA polymerase (Invitrogen). DNA sequencing of the coding exons and intronic flanking regions was performed by the fluorometric method on both strands (ABI BigDye Terminator Sequencing Kit V.2.1, Applied Biosystems). We sequenced the *GPC5* coding sequence and flanking introns, the miR-17~92 cluster (chr13:92,002,859–92,003,645) (primers are listed in **Supplementary Table 2**) and the putative miR-17a and miR-20a binding site in the 3′ untranslated region of *MYCN* (chr2:16,087,062–16,087,085) in the eight individuals with Feingold syndrome with no chromosomal rearrangements.

34. Cognet, M. *et al.* Dissection of the MYCN locus in Feingold syndrome and isolated oesophageal atresia. *Eur. J. Hum. Genet.* **19**, 602–606 (2011).
35. Masurel-Paulet, A. *et al.* Delineation of 15q13.3 microdeletions. *Clin. Genet.* **78**, 149–161 (2010).

doi:10.1038/ng.915